Underwater Channel Characteristics and Wireless Optical Communications Using a Blue Mode-Locked Semiconductor Disk Laser

Liqi Liu, Tao Wang, Ruiyang Tian, Renjiang Zhu, Cunzhu Tong, *Senior Member, IEEE*, Lijie Wang, Yanrong Song, and Peng Zhang

***Abstract*—An advanced light source at blue-green waveband is the key to improve the link-distance and communication performance of an underwater wireless optical communication (UWOC) system. This work presents the underwater channel characteristics and UWOC system using a blue semiconductor disk laser that passively mode-locked by a semiconductor saturable absorb mirror for the first time. The attenuation coefficients of the continuous-wave and mode-locked lasers under different concentrations of Maalox solution are studied, and the results indicate that the attenuation coefficients of the mode-locked laser are obviously lower than that of the continuous-wave laser. Then an UWOC system based on an acousto-optic modulator are constructed, and the water tank communication experiments are carried out by using quasi-cyclic low-density-parity-check coding and 64-pulse-position-modulation. Experimental results show that the bit error rates of the mode-locked laser are significantly lower than that of continuous-wave laser under the same Maalox solution concentration and same signal-noise-ratio. These results provide an attractive light source for practical long-distance UWOC.**

***Index Terms*—Acousto-optic modulator, mode-locked, pulse position modulation, quasi-cyclic low-density-parity-check, semiconductor disk laser, underwater wireless optical communication.**

Manuscript received 17 December 2022; revised 15 February 2023 and 20 March 2023; accepted 23 March 2023. Date of publication 28 March 2023; date of current version 16 August 2023. This work was supported in part by the National Natural Science Foundation of China under Grant 61904024, in part by the Cooperation Project between Chongqing Local Universities and Institutions of Chinese Academy of Sciences, Chongqing Municipal Education Commission under Grant HZ2021007, in part by the National Natural Science Foundation of China under Grants 61975003, 61790584, and 62025506, in part by the Science and Technology Research Program of Chongqing Municipal Education Commission under Grant KJZD-M201900502, and in part by the State Key Laboratory of Luminescence and Applications under Grant SKLA-2019-04. *(Corresponding authors: Tao Wang; Peng Zhang.)*

Liqi Liu, Tao Wang, Ruiyang Tian, and Renjiang Zhu are with the College of Physics and Electronic Engineering, Chongqing Normal University, Chongqing 401331, China (e-mail: 2020110511017@stu.cqnu.edu.cn; wangt@cqnu.edu.cn; 2687020480@qq.com; 20131121@cqnu.edu.cn).

Cunzhu Tong and Lijie Wang are with the Changchun Institute of Optics, Fine Mechanics and Physics, Chinese Academy of Sciences, Jilin 130033, China (e-mail: tongcz@ciomp.ac.cn; wanglijie@ciomp.ac.cn).

Yanrong Song is with the College of Applied Sciences, Beijing University of Technology, Beijing 100124, China (e-mail: yrsong@bjut.edu.cn).

Peng Zhang is with the National Center for Applied Mathematics in Chongqing, Chongqing Normal University, Chongqing 401331, China (e-mail: zhangpeng2010@cqnu.edu.cn).

Color versions of one or more figures in this article are available at https://doi.org/10.1109/JLT.2023.3262683.

Digital Object Identifier 10.1109/JLT.2023.3262683

I. Introduction

TRADITIONAL means of underwater communications, i.e., acoustic and radio frequency (RF) communications, have been unable to meet the increased needs of ocean activities and researches. Underwater acoustic communication cannot achieve high transmission rate because of its low bandwidth, while RF communication cannot realize long-distance link underwater since its serious attenuation. On the contrary, underwater wireless optical communication (UWOC) has become a promising method for many researchers because of its advantages of low delay, long-distance link, high bandwidth, small device size and good security [1], [2], [3]. It provides an efficient and practical communication pattern for underwater wireless sensor networks composed of seabed sensors, relay buoys, autonomous underwater vehicles, and remotely operated vehicles [4].

So far, many works on UWOC have been reported for improving the transmission distance, data rate, and anti-interference capability along the underwater links. By using a 520 nm LD light source, On-Off Keying (OOK) modulation and linear equalization method, Wang reported a 100 m/500-Mbps UWOC system in 2019 [5]. In 2020, Yang et al. demonstrated a 100 m/100-Mbps UWOC system using a high-power frequency-doubled 532 nm green laser from a 1064 nm continuous-wave (CW) solid-state laser [6]. In 2021, Chen demonstrated a 150-m/500-Mbps UWOC system by employing partial response shaping, interleaving, precoding, and lattice coded modulation technology [7]. In 2022, Chao et al. realized a 100 m/3-Gbps UWOC system by using a photomultiplier [8]. However, with the increase of communication distance, the waveform of signal begins to deform, which makes it necessary to use more complex coding and shaping technology on the transmitter or receiver. Compared with OOK or pulse amplitude modulation (PAM), for a given bit error rate (BER), the format of pulse phase modulation signal (such as pulse position modulation (PPM) [9], differential pulse position modulation (DPPM), digital pulse interval modulation (DPIM)) has higher power efficiency and better anti-noise performance. Among the PPM, DPPM and DPIM [10], the PPM is the easiest way to implement, and has been widely used in a UWOC system. It has become the modulation format selected by most researchers.

TABLE I
RESEARCHES OF M-PPM UWOC SYSTEM

Years/Months	Institutions	Light source	Data rate	Distance (m)	Detector	Modulation	Ref.
2018.08	SIOM[a]	LD	1.7 MHz	120	SPAD	256-PPM	[17]
2018.08	ZJU[b]	LD	5 MHz	46	MPPC	4-PPM	[11]
2021.09	NCU[c]	LED	5 MHz	1.5	SPAD	256-PPM	[12]
2021.10	SITP[d]	LD	6.21 MHz	2	SPAD	4-PPM	[13]
2022.08	ZJU[b]	MOPA	9.14 MHz	99	PMT	64-PPM	[14]
2022.10	SUSTech[e]	LED	50 MHz	2	APD	8-PPM	[15]
2022.10	ZJU[b]	LD	200 ps	7	PD	64-PPM	[16]
2023	CQNU[f]	SDL	4.69 MHz	18	APD	64-PPM	This work

[a]SIOM: Shanghai Institute of Optics and Fine Mechanics
[b]ZJU: Zhejiang University
[c]NCU: Nanchang University
[d]SITP: Shanghai Institute of Technical Physics
[e]SUSTech: Southern University of Science and Technology
[f]CQNU: Chongqing Normal University

Table I lists the research progress of PPM modulated UWOC system in recent years. In 2018, Shen et al. implemented a UWOC system with a link-distance of 46 m by utilizing the power efficient PPM and ultra-sensitive multi-pixel photon counter [11]. In subsequent studies, most researchers used single photon or weak light detection [12], [13], [14], [15], [16].

When most researches focused on the efficient modulation, advanced coding, and weak-light detection to achieve long-distance transmission, there was few investigations about the light source used in a UWOC system. The pulsed laser was used by Hu et al. who used 256-PPM. They reported a UWOC system with 13.7 MHz bandwidth, 35.88 attenuation length and 120 m transmission distance in Jerlov II water [17]. However, their PPM pulse signal needs to adapt to low repetition rate (1.5 KHz), which brings inconvenience to their research. Therefore, an efficient UWOC light source is the premise to realize long-distance communication.

Light sources commonly used in UWOC are light-emitting diodes (LEDs) and laser diodes (LDs). LED can only be used in underwater sensor networks because of its large divergence and low bandwidth. LD has become the preferred light source for long-distance communication in virtue of its small beam divergence and high bandwidth [18]. One of the most important measures to improve the performance of a UWOC system is a high-quality blue light source which experiences the lowest absorption coefficient in ocean [19], [20].

Semiconductor lasers have advantages of high efficiency, long life, small volume, high integration capacity compared with dye lasers and solid-state lasers, but it is difficult for a semiconductor laser to obtain high power and good beam quality at the same time. The output power of an edge-emitting semiconductor laser has exceeded 10 W, however, the laser works with multi-transverse modes and poor beam quality. Although vertical-cavity surface-emitting laser can produce excellent beam quality, its output power is limited to milliwatts.

Semiconductor disk lasers (SDLs), or named as optically-pumped vertical-external-cavity surface-emitting lasers (VECSELs) have attracted attention in academia and industry for its ability to produce high output power and good beam quality simultaneously [21], [22], [23], [24]. The reported output power of a VECSEL with fundamental transverse mode has been more than 20 W, and the M^2 factor of beam quality was about 1.1 [25]. The demonstrated maximum output power of a multiple transverse mode VECSEL has exceeded 100 W [26]. Most importantly, its emission wavelength can be designed according to actual applications by the bandgap engineering, and using nonlinear frequency conversion, its emission wavelength can be further extended to the wide range from ultraviolet to mid-infrared, which includes the desired blue-green waveband for UWOC.

In 1963, Duntley et al. found that the absorption coefficient of 450–550 nm light in seawater was much lower than that of the other visible light. Even in the blue-green waveband with relatively weak absorption, attenuation coefficients of seawater to laser beams at different wavelengths changes significantly with the various wavelength. Therefore, a light source with suitable wavelength is one of the most important things for long-distance transmission.

Because of the portability and operability of the internal modulation (i.e., direct modulation), it appears in most of the reported UWOC systems. By changing the injected current of the laser, internal modulation transfers the electronic signals to a light wave. Since it is difficult to modulate the large driving current of a high-power semiconductor laser, output power of a commercially available directly-modulated laser is limited to tens of milliwatts. Although advanced detector, e.g., single-photon detector, can extend the link distance beyond 100 meters, finding single photons in ocean is a huge challenge for engineering applications.

Therefore, external modulation is an attractive and alternative means. As a typical external modulator, acousto-optic modulator (AOM) changes the amplitude of diffraction light when the laser beam passes through the ultrasonic field (which is determined by the electronic signal that loaded on the piezoelectric transducer) in the acousto-optic crystal (generally, lithium niobate), so to transfers the electronic signals to a light wave. It pushes the

output power of a light source from tens of milliwatts to several watts without affecting the stability of the resonant cavity of the light source, and can significantly upgrade the communication distance at MHz data rate, which is three orders of magnitude bigger than that of acoustic communication and can meet the needs of most applications of UWOC.

In this work, we use a frequency-doubled 490 nm SDL that mode-locked (ML) by a semiconductor saturable absorption mirror (SESAM) as the light source of UWOC. And the frequency-doubled 490 nm CW SDL is also built through the same gain chip. By measuring the attenuation of the CW and ML blue SDL in different underwater channels, the channel characteristics of the above two different lasers are investigated. Then, an AOM based UWOC system using quasi-cyclic low-density-parity-check (QC-LDPC) coding and 64-PPM is built. Experimental results show that ML laser has smaller attenuation and bit error rate (BER) than the CW laser in the same water quality. And in the case of low signal noise ratio (SNR), ML laser shows better communication quality than the CW laser.

II. Blue Mode-Locked Semiconductor Disk Laser

Compared with CW lasers, a ML laser can produce high peak power and could suffer smaller attenuation, thus support longer link distance of a UWOC system. Gain chip for the blue mode-locked SDL is epitaxially grown in reverse sequences as: the AlGaAs etch stop layer with high Al composition, the GaAs protect layer, the AlGaAs window layer with high barrier, the active region, the distributed Bragg reflector (DBR) and the antioxidant GaAs cap layer. There are 15 InGaAs/GaAsP quantum wells in the active region, the content of In in InGaAs well layer is designed to meet the target laser wavelength of 980 nm, and the content of P in GaAsP barrier layer (also works as the strain compensation layer) must be adequate to compensate the strain but not too much to absorb the pumping energy. The DBR is composed of 30 pairs alternate AlGaAs layers with high Al (lower refractive index) and low Al (higher refractive index) composition, and the designed center wavelength and high-reflectivity bandwidth of it are 980 nm and 100 nm respectively. According to the test data given by the manufacturer, the reflectivity of DBR at 980 nm wavelength is about 99%. The DBR reflectivity, the surface emitting photoluminescence (PL) and the laser spectrum are shown in Fig. 1.

When the grown wafer is split to small chips with 4 mm×4 mm dimension, the epitaxial end face is metalized with titanium-platinum-gold sequentially, then the chip is bonded to a copper heatsink, and the substrate is removed using chemical etch. The experimental setup of our ML blue SDL is shown in Fig. 2. The heatsink is mounted to a thermal-electronic cooler, which is then connected with a water-cooling system to keep the temperature at 15 °C. A V-shaped resonant cavity is formed by the DBR at bottom of gain chip and another DBR at bottom of SESAM, and a folded mirror with 50 mm radius of curvature and 99.9% reflectivity at 980 nm is used as the output coupler. The pump source is an 808 nm fiber-coupled semiconductor diode laser with 11.5 W output power, and the core diameter of its pigtail fiber is 100 μm. We use a 1:1 imaging lens pair

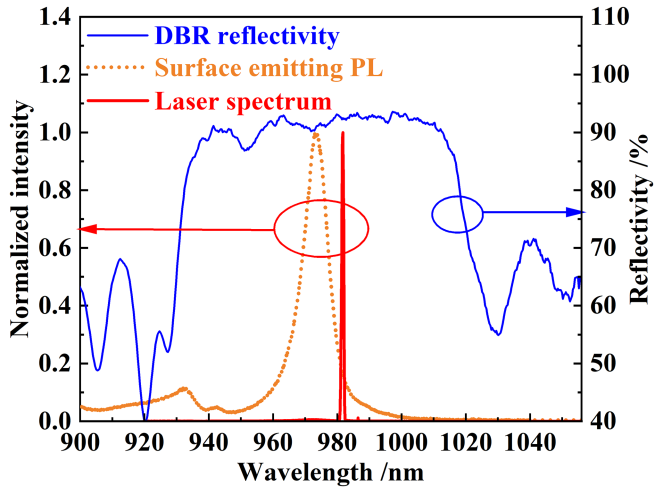

Fig. 1. Measured DBR reflectivity, surface emitting photoluminescence (PL) and laser spectrum.

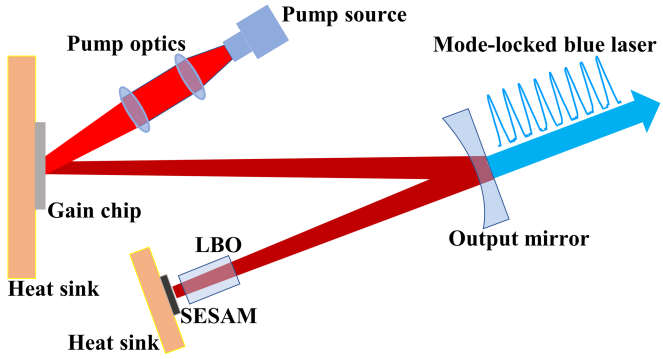

Fig. 2. Schematics of the CW and the SESAM mode-locked blue SDL.

to focus the pump beam on gain chip at an incident angle of about 30°, and this will deliver a pump spot with diameter of about 100 μm on gain chip, approximately matching to the laser spot.

To start mode-locking, the lengths of arms including gain chip and SESAM are selected to be 65 and 38 mm respectively, so to obtain the ratio of spot area on the gain chip and SESAM of about 25:1. With the above ratio, SESAM can be saturated prior to the gain, and the saturated loss of SESAM and the successively saturated gain will form a net gain window, in which a laser pulse can be built. By slightly adjusting the output coupler or fine tuning the length between the output coupler and SESAM, stable continuous-wave mode-locking can be produced. A high-speed free space detector (Thorlabs DET08C, 5 GHz bandwidth, 800–1700 nm waveband) is used to receive the output pulses, and the signal is delivered to a mixed signal oscilloscope (Tektronix MSO68B, 10 GHz bandwidth, 50 GHz sampling frequency) for showing the pulse train. The observed mode-locked pulse train is plotted in Fig. 3, and the inset indicates pulses in 200 ns time range.

The repetition rate of mode-locked pulses is recorded by a spectrum analyzer (RIGOL DSA800, 7.5 GHz bandwidth), and

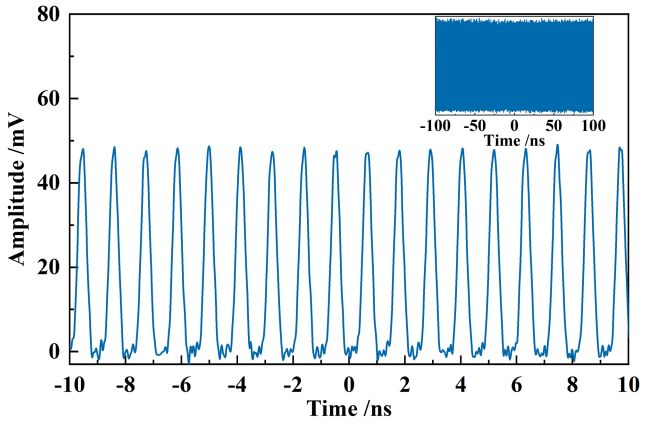

Fig. 3. Pulse train of the continuous-wave mode-locked SDL. The inset shows pulses in 200 ns time range.

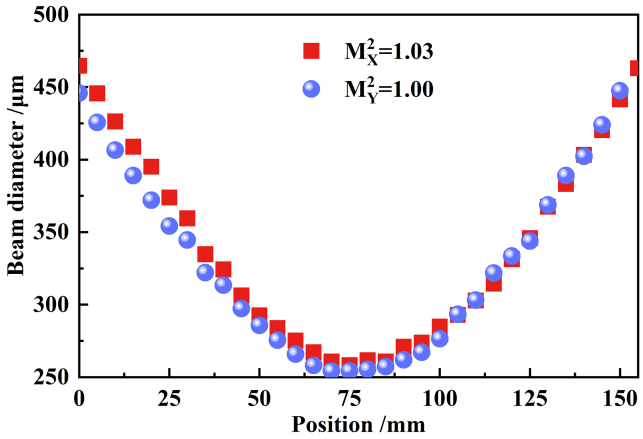

Fig. 5. Measured M2 factor of the output beam of the mode-locked SDL.

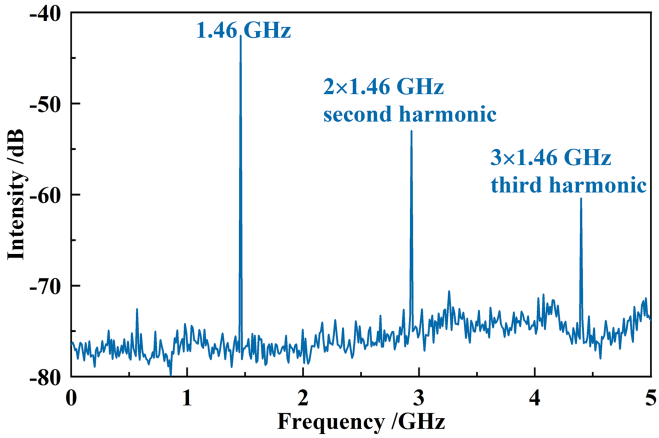

Fig. 4. RF spectra of the mode-locked SDL. The second and the third harmonic are also plotted.

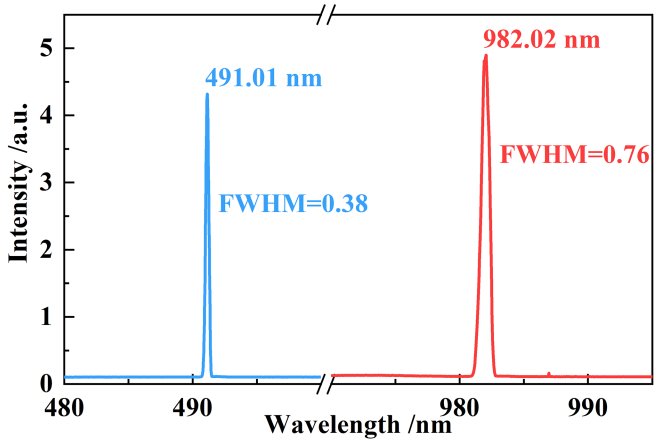

Fig. 6. Spectra of the frequency-doubled mode-locked SDL.

the measured RF spectra can be found in Fig. 4. The fundamental signal of 1.46 GHz is strictly corresponding to the cavity length of 103 mm. We also measure the beam quality of the ML laser using a M^2 measurement system (Thorlabs M2MS-BC106N), and the results are shown in Fig. 5. The M^2 factors on x and y directions are 1.03 and 1.00 respectively, indicating a good beam quality of the SESAM mode-locked SDL.

After the achievement of stable mode-locking, a 5 mm length lithium borate (LBO) crystal is inserted in the arm that include the SESAM for frequency-doubling. The crystal should be situated close to the SESAM as can as possible, so to produce a smaller laser spot on crystal and obtain higher conversion efficiency of frequency-doubling. It should be noted that the inserted crystal may destroy previously mode-locking, and some further adjustments of the cavity are needed to maintain the mode-locking. When the position of the SESAM was adjusted properly, the mode-locked light can be obtained. Spectra of the frequency-doubled mode-locked SDL are measured using a spectrometer (HORIBA iHR320, 150–1500 nm wavelength range, 0.06 nm resolution) and the wavelength and linewidth of the CW blue light and the mode-locked blue light are shown together in Fig. 6. At the same time, for the comparability of the experimental results, we also ensure that the power of the CW blue laser and the mode-locked blue laser are the same.

III. Underwater Channel Characteristics

Even the cleanest water attenuates light severely. The quantitative characterization of the decay of light underwater can be determined by the Beer-Lambert law [27], [28], [29]:

$$P_T(\lambda) = P_I(\lambda)e^{-c(\lambda)l} \tag{1}$$

where $P_I(\lambda)$ and $P_T(\lambda)$ represent the transmitted and received powers of the light, c is the attenuation coefficient, and l is the channel distance. The attenuation coefficient, which is defined as attenuation of optical power per meter, can be extracted from (1) and expressed as:

$$c = -\frac{\ln \frac{P_I(\lambda)}{P_T(\lambda)}}{l} \tag{2}$$

Since the attenuation of light in water is caused by two independent physical processes (absorption and scattering), the

attenuation coefficient c has the following formula:

$$c = a(\lambda) + b(\lambda) \tag{3}$$

$a(\lambda)$ and $b(\lambda)$ are the absorption and scattering coefficient, the two intrinsic parameters that often used to characterize the optical properties of medium.

Obviously, attenuation caused by scattering from water, dissolved materials and non-algal suspended particles is the problem restricting long-distance underwater communication. These scattering cause the collimated beam to diverge, making more photons to annihilate in transmission. With the development of light source, photoelectric detection and receiving technology, some researches has been done by using high frequency modulation to investigate the scattering of light in water. In 2009, Linda et al. conducted underwater scattering experiments using a 532 nm ML laser, and found that the forward scattering was reduced with an increased repetition rate of the laser pulse [30]. Their works in 2017 also showed that light wave with higher modulation frequency suffered less loss from forward scattering [31]. Other theoretical researches also indicated that the angular distribution of forward scattered light decreases with the increase of modulation frequency [32], [33], which were consistent with the above experimental results.

Scattering in seawater can be divided into Rayleigh scattering and Mie scattering. Generally, only Rayleigh scattering needs to be considered in pure water or underwater environment with few impurities. In seawater containing various impurities, both Rayleigh scattering and Mie scattering should be considered. To study the scattering, Maalox suspension solution is chosen in the experiments to take the place of seawater. This is a mixed solution of Al $(OH)_3$ (220 mg/5 ml) and Mg $(OH)_2$ (195 mg/5 ml) as the main component. We put 20 ml mixed solution into the water tank (with 0.073 m^3 water) each time to prepare underwater channel with different scattering concentrations, and the prepared concentrations are 0, 115.3, 230.5, 345.8 and 461.1 $mg{\cdot}m^{-3}$.

Then the blue ML laser and CW laser described in section 2 with 15.6 mW average power are used to study the underwater channel characteristics. The blue laser passes through a 1.5 m $\times$ 0.4 m $\times$ 0.3 m water tank, and the total 18 m length optical path is formed as shown in Fig. 11. A 250 mm $\times$ 100 mm bigger mirror is used on one side, and five 20 mm $\times$ 20 mm smaller mirrors are put on the other side in order to facilitate the adjustment of the light path. A beam expander composed of two plane-convex lenses with 75 mm and 300 mm focal length has been designed and put in front of the water tank, and the power of output laser beam is measured by a power meter (Thorlabs PM100D) with a detector (Thorlabs S140C, 5 mm aperture, 350–1100 nm wavelength, 0.001–500 mW power range).

The output light power is measured at different transmission distances and various water quality with changed concentration of Maalox suspension solution, and the corresponding power attenuation curves of the ML laser are shown in Fig. 7. The respective slope is marked on the right side of every curves. It can be concluded from Fig. 7 that the power (in dBm) decreases linearly with the increasing distance, and the absolute value of slope of attenuation curve increase with the increased concentration. That is, light with same power can transmit farther distance in water with smaller concentration.

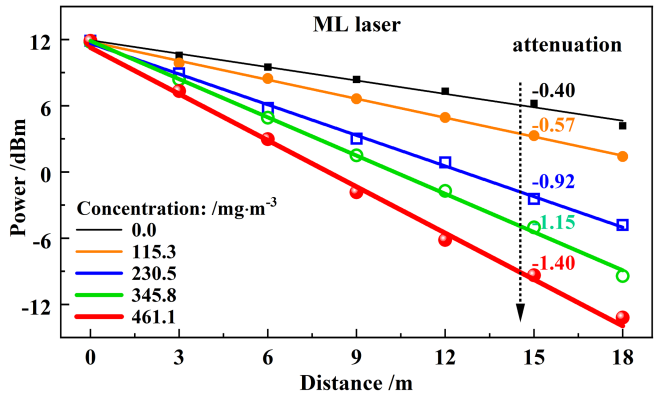

Fig. 7. Power attenuation of the ML laser with different distance.

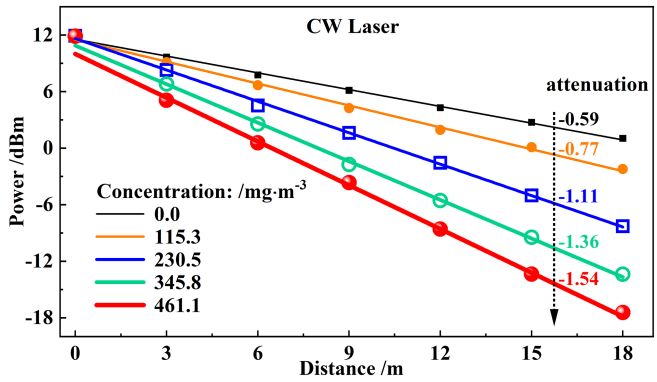

Fig. 8. Power attenuation of the CW laser with different distance.

On comparison, we plot the power attenuation curves of a CW laser under different Maalox solution concentration in Fig. 8. Similar to Fig. 7, the power decreases linearly with the increasing distance, and the absolute value of slope of attenuation curve increase with the increased concentration. The difference of Figs. 7 and 8 is that the slope of attenuation curve of the CW laser is always bigger than that of the ML laser.

Power attenuation of ML and CW laser are put together in Fig. 9. It can be seen from Fig. 9 that the powers of ML laser are always higher than that of CW laser at the same distance with different concentration. After 18 m transmission distance, under 0 $mg{\cdot}m^{-3}$, 203.5 $mg{\cdot}m^{-3}$ and 461.1 $mg{\cdot}m^{-3}$ concentrations, the powers of ML and CW laser are 4.18 and 1.03 dBm, -4.81 and -8.29 dBm, -13.18 and -17.44 dBm. Obviously, with increased concentration (i.e., 0, 203.5 and 461.1 $mg{\cdot}m^{-3}$), the power difference (3.15, 3.48 and 4.36 dBm) between ML and CW laser increases gradually, and this means that the advantage of ML laser is more significant under higher concentration (i.e., more intensive scattering).

Values of different distance and the corresponding powers in Figs. 7 and 8 are substituted into (2), and the calculated attenuation coefficients are plotted in Fig. 10. It can be seen

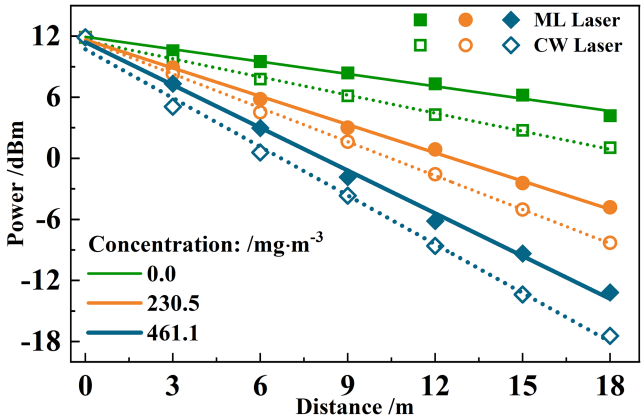

Fig. 9. Comparison of the attenuation curves of the ML and the CW lasers.

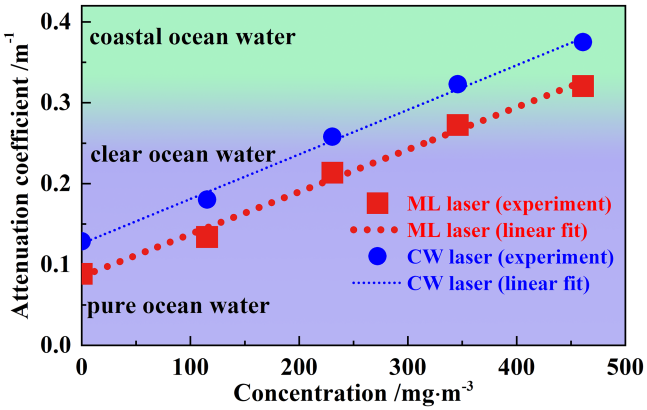

Fig. 10. Attenuation coefficients of the ML and the CW lasers.

the attenuation coefficient increase linearly with the increased concentration, and ML laser always has lower attenuation coefficient than CW laser. For example, when the concentration is 0 mg·m^{-3}, attenuation coefficient of CW laser is 0.128 m^{-1}, and the power required for 100 m transmission will be 3.6 W (given the received power of 0.01 mW). On contrast, attenuation coefficient of ML laser is 0.08 m^{-1}, 3.6 W could transmit about 160 m, 60 m further than CW laser. Even increase the power of CW laser by 10 dB, which is a huge challenge for engineering realization, the transmission distance only could be pushed to 118 m, still shorter than 160 m of the ML laser.

We mark the attenuation coefficients of three common water types, i.e., pure ocean water (c = 0.0641 m^{-1}), clear ocean water (c = 0.1502 m^{-1}) and coastal ocean water (c = 0.399 m^{-1}). The attenuation coefficients of CW laser in Fig. 10 are same as reported values by Tian et al. [29], but attenuation coefficients of ML laser are significantly smaller than that of CW laser.

For a pulsed light beam, it has been reported that when the intensity of laser exceeds the threshold of underwater nonlinear optics (~10^8–10^9 W/cm^2), strong nonlinear processes such as stimulated Brillouin scattering, stimulated Raman scattering and stimulated heat scattering will occur, and this would result in dramatical change of the attenuation coefficient of light in water [34]. In this work, the light intensity of the used blue mode-locked SDL is estimated to be about 1.7 × 10^3 W/cm^2,

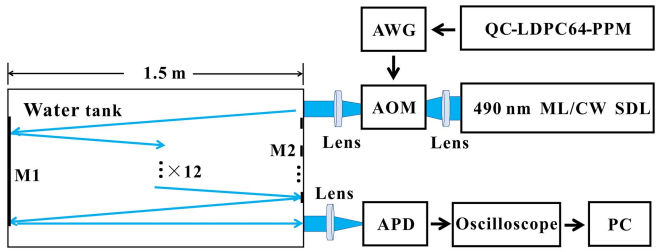

Fig. 11. Experimental setup of the UWOC system using blue ML/CW SDL. M1: Mirror1, M2: Mirrors2.

far smaller than the threshold of underwater nonlinear optics mentioned above, so the reduction of attenuation coefficient of the ML laser cannot be caused by nonlinear effects. We think that the ML laser pulses train with high repetition rate can be regarded as high frequency modulated light wave, which will suffer lower scattering attenuation underwater, just as reported in references [30], [31], [32], [33].

IV. UWOC System

To further utilize the idea underwater channel characteristics of the ML laser, we introduce our frequency-doubled SESAM mode-locked SDL into a UWOC system and compare its performance with a continuous-wave SDL. An AOM, whose feasibility for UWOC has been verified by our previous work [35], was selected as the modulator in this experiment.

The blue ML/CW SDL based UWOC experimental system using QC-LDPC coding and 64-PPM modulation is shown in Fig. 11. The 64-PPM modulation signal with QC-LDPC coding is loaded into an arbitrary waveform generator (AWG) (Tektronix AWG70002A, 50 Gs/s sampling rate, 2 Gs record length) for digital-to-analog conversion, and is transferred to analog signal. This analog signal is then delivered to the driver of AOM, in which the incident light beam is modulated by the analogy signal. A lens with shorter focal length (f_1 = 75 mm) is used to focus the 490 nm blue laser before it entering the AOM, and another lens with longer focal length (f_2 = 300 mm) is employed on the other side to expand the laser beam to reduce its divergence. The modulated laser beam passes through the water tank and the total length of underwater communication link is about 18 m. The output beam is focused by a lens onto an avalanche photodetector (Thorlabs APD210, 400–1000 nm wavelength range, 5–1600 MHz bandwidth), and a mixed signal oscilloscope is used to record and analyze the received signal. All experiments are carried out in dark environment to minimize the influence of light noise.

Fig. 12 shows the key parts of the UWOC system. Fig. 12(a) shows the transmitter including a ML/CW laser (with an 808 nm pump source, gain chip, SESAM, LBO), an AOM and a pair of lenses. Fig. 12(b) shows the underwater communication link and receiver equipment.

There are many modulation methods that can be used in UWOC. OOK modulation is widely used as one of the earliest modulation modes, and is relatively easy to implement. But

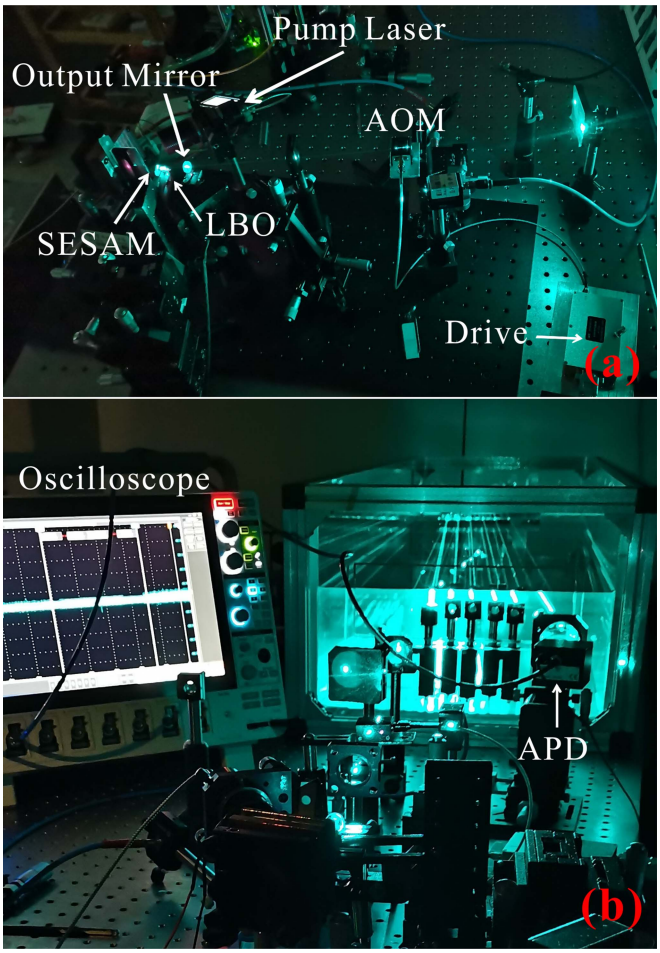

Fig. 12. Key parts of the UWOC system using blue ML/CW SDL. (a) The transmitter including a ML/CW laser, an AOM and a pair of lenses. (b) The underwater optical link. And the receiver containing a focusing lens, an APD and an oscilloscope.

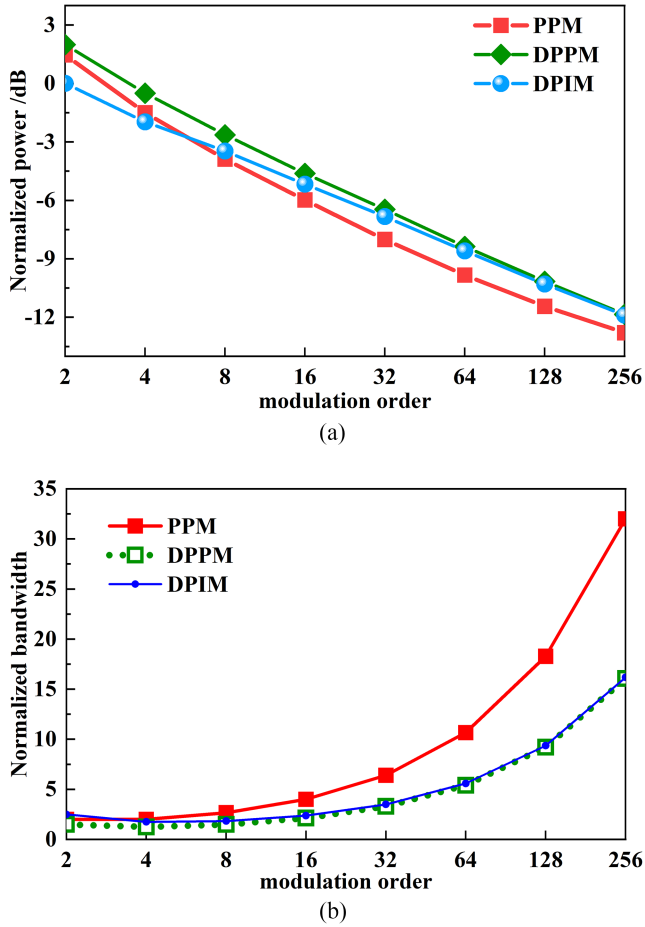

Fig. 13. Normalized powers (a) and normalized bandwidths (b) with various modulation orders under PPM, DPPM and DPIM.

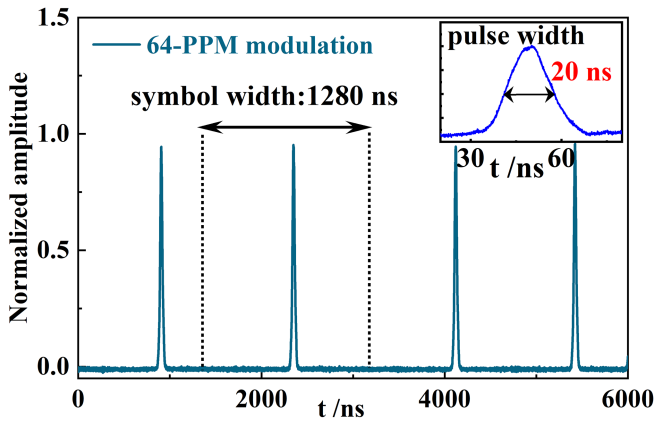

Fig. 14. Transmitted characterization with 64-PPM modulation.

compared with others modulation methods, its power utilization is not so good. PPM is a modulation mode that transmits information by using the relative position of pulse. In optical communication, PPM modulation method can achieve high data transmission rate with the lowest average optical power [36]. DPPM removes those zeros after the high-level pulse in PPM, it is an improved version of PPM. DPIM uses the relative distance between two neighbor pulses to transmit information.

The modulation and demodulation mode of information play an important role in a communication system. On the premise of reliability, the modulation mode with high transmission rate (the amount of information transmitted per unit time) or high transmission efficiency (the amount of information transmitted per unit energy) should be selected. In our UWOC, the selected 64-PPM can take both transmission rate and efficiency into account. The communication quality is tested using 64-PPM modulation with 1/2 code rate QC-LDPC code, and the error code analysis is performed on the generated 2^{16}-1 symbols at different distances (0–18 m) and Maalox suspension solution concentrations. The power attenuation is shown in Figs. 7 and 8. Considering the limited bandwidth of AOM, the possible shortest pulse width of 20 ns is used in the above experiments in Fig. 14. At the same time, to ensure the comparability of the experiment, we have ensured that the average power of ML and CW lasers are both 15.6 mW.

Fig. 15 shows the communication performance of ML and CW laser with and without QC-LDPC coding at 18 m distance. Obviously, BERs increase with the increased concentration of

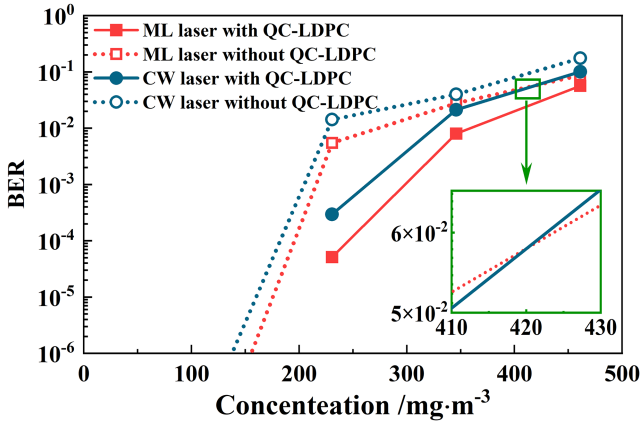

Fig. 15. BERs at different Maalox concentrations. The inset at the bottom right shows the enlargement of the marked area.

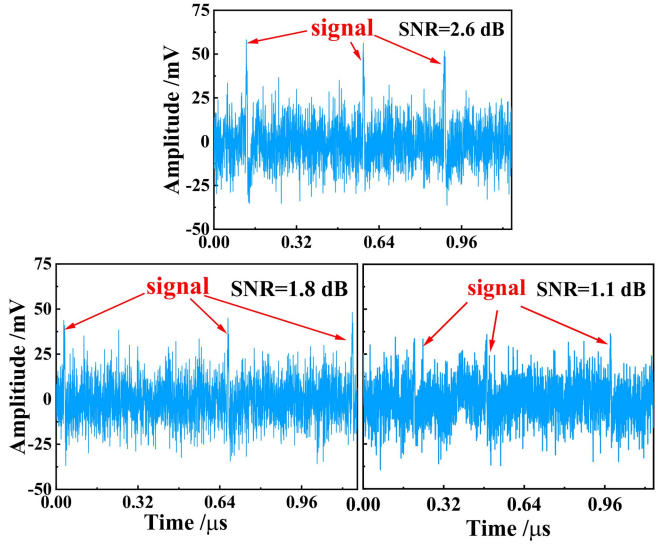

Fig. 16. Waveforms of the received signal and noise under three different SNR.

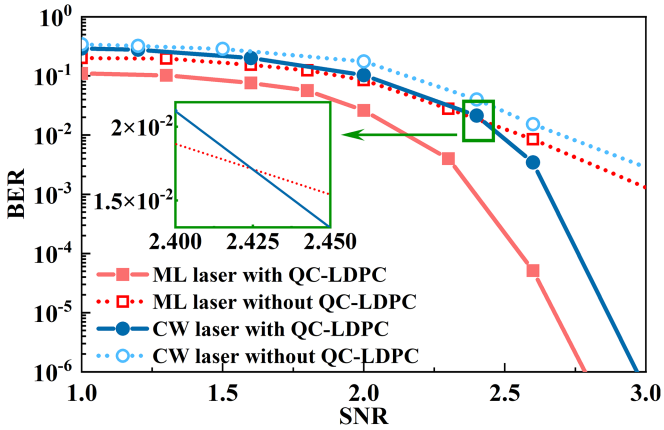

Fig. 17. BERs versus SNRs of ML and CW lasers with and without QC-LDPC coding. The inset at the bottom left shows the enlargement of the marked area.

Maalox solution, and this is understandable: higher concentration aggravates the forward and back scattering underwater, and the folded optical path further increase the interference between light beams. Both above factors will decrease the signal-to-noise ratio and increase the BER. At 0 mg·m^{-3} and 115.3 mg·m^{-3} Maalox solution concentrations, the BERs of ML and CW lasers without QC-LDPC are much lower than 10^{-5}, and the BERs of ML and CW lasers with QC-LDPC are all zeros, so they are not plotted in the Fig. 14.

At 230.6 mg·m^{-3} concentrations, BERs of ML and CW laser with QC-LDPC coding are 5.12×10^{-5} and 2.94×10^{-4}, while BERs of ML and CW laser without QC-LDPC coding are 5.48×10^{-3} and 1.42×10^{-2}. It can be concluded that for the same laser, with QC-LDPC coding has lower BER than without QC-LDPC coding; and for the same coding, ML laser has lower BER than CW laser. It should be noted that at the concentration of 461.1 mg·m^{-3}, BER of the ML laser without QC-LDPC is 8.6×10^{-2}, already lower than that of the CW laser with QC-LDPC coding (9.8×10^{-2}), and this indicate that the ML laser has more obvious advantage at high Maalox solution concentrations, i.e., high scattering concentration.

Then we add more Maalox solution into the water tank to obtain higher concentration beyond 461.1 mg·m^{-3}, to discuss BERs of ML and CW laser under higher scattering (lower SNR) condition in detail. Fig. 16 shows the waveforms of the received signal and noise under three different SNRs.

The relationships between SNRs and BERs of ML and CW lasers are shown in Fig. 17. It is clear that the BERs increase with the decreasing SNRs. It can be seen from Fig. 17 that under low SNR (<3 dB), only the BER of ML laser with QC-LDPC is in the order of 10^{-4}, which is not only at least one order of magnitude lower than other cases, but also below the threshold BER of effective communication (i.e., below forward error correction threshold of 3.8×10^{-3}). It also can be seen from Fig. 16 that when the SNR is less than 2.425 dB, BERs of ML laser without QC-LDPC coding are lower than that of CW laser with QC-LDPC coding, and this shows again that ML laser has better performance under high scattering conditions, e.g., costal ocean water.

V. Discussions

The ML laser used in the experiment has the same output power as the CW laser. The only difference between them is that the peak power of the ML laser pulse is two orders of magnitude higher than the output power of the CW laser. The experimental results show that the attenuation coefficient of the ML laser is significantly smaller than that of CW laser in any water quality. Theoretically, the attenuation coefficient of light in water is independent of its power, so the high peak power of ML lasers is not the direct reason for their small attenuation coefficient. At the same time, the peak power of the ML laser used in the experiment has not yet reached the conditions for generating nonlinear effects in water, so the influence of nonlinear effects on reducing the attenuation coefficient can also be ignored. The remaining reasonable explanation is that the high repetition rate of the ML laser result in a decrease in its attenuation coefficient. In fact, the pulse train of the ML laser can be considered as a modulated light wave. It should be noted that

high-frequency modulated light waves can significantly reduce their forward scattering in water, which has been reported in the early literature. Obviously, a reduced forward scattering means a smaller attenuation coefficient. Therefore, we believe that the high repetition rate of the ML laser pulse results in a significantly smaller attenuation coefficient in water compared with the CW laser.

QC-LDPC is a type of error-correction code that can effectively solve the increasing BER caused by sudden errors in transmission. In UWOC, the above increasing BER are inevitable, so the QC-LDPC coding can significantly reduce the BER and improve communication performance. In this article, for both ML and CW laser, QC-LDPC has an obvious effect on reducing BER. By comparison, we found that even without the beneficial coding method of QC-LDPC, the BER of the ML laser would be lower than that of the CW laser. Especially under high scattering conditions, the performance of the ML lasers is more prominent. When the scattering coefficient reaches a certain value, so that the CW laser can no longer meet the communication requirements, the ML laser can still do well.

VI. Conclusion

In summary, by using a frequency-doubled 490 nm SDL that passively mode-locked by a SESAM, we have measured the attenuation coefficients of the ML laser and compared it with the case of CW laser under different concentrations of Maalox solution. Experimental results show that the ML laser has obviously lower attenuation coefficient than that of CW laser. and Based on the ML/CW blue SDL, along with an AOM, we also have demonstrated a UWOC system using QC-LDPC and 64-PPM. BERs of the ML/CW lasers with and without QC-LDPC under different Maalox solution concentrations are investigated, and it can be concluded that the BERs of the ML laser are significantly lower than that of CW laser. BERs of the ML/CW lasers with and without QC-LDPC under high Maalox solution (i.e., low SNR) are studied particularly, and the ML laser shows much better performance than the CW laser. Especially, BERs of the ML laser without QC-LDPC become lower than that of CW laser with QC-LDPC, which further verify the advantage of the ML laser as a light source for UWOC.

References

[1] J. Li, D. Ye, K. Fu, L. Wang, J. Piao, and Y. Wang, "Single-photon detection for MIMO underwater wireless optical communication enabled by arrayed leds and SiPMs," *Opt. Exp.*, vol. 29, no. 16, pp. 25922–25944, Jul. 2021.

[2] B. D. Deebak and F. Al-Turjman, "Aerial and underwater drone communication: Potentials and vulnerabilities," in *Drones in Smart-Cities*. Amsterdam, The Netherlands: Elsevier, Jun. 2020, pp. 1–26.

[3] Z. Zeng, S. Fu, H. Zhang, Y. Dong, and J. Cheng, "A survey of underwater optical wireless communications," *IEEE Commun. Surv. Tut.*, vol. 19, no. 1, pp. 204–238, Firstquarter 2017.

[4] M. Singh, M. L. Singh, G. Singh, H. Kaur, and S. Kaur, "Real-time image transmission through underwater wireless optical communication link for internet of underwater things," *Int. J. Commun. Syst.*, vol. 34, no. 16, Aug. 2021, Art. no. e4951.

[5] J. Wang, C. Lu, S. Li, and Z. Xu, "100 m/500 Mbps underwater optical wireless communication using an NRZ-OOK modulated 520 nm laser diode," *Opt. Exp.*, vol. 27, no. 9, pp. 12171–12181, Apr. 2019.

[6] Y. Yang et al., "Long-distance underwater optical wireless communication with PPLN wavelength conversion," *Proc. SPIE*, vol. 11717, pp. 639–646, 2020.

[7] X. Chen et al., "150 m/500 Mbps underwater wireless optical communication enabled by sensitive detection and the combination of receiver-side partial response shaping and TCM technology," *J. Lightw. Technol.*, vol. 39, no. 14, pp. 4614–4621, Jul. 2021.

[8] C. Fei et al., "100-m/3-Gbps underwater wireless optical transmission using a wideband photomultiplier tube (PMT)," *Opt. Exp.*, vol. 30, no. 2, pp. 2326–2337, Jan. 2022.

[9] T. Y. Elganimi, "Performance comparison between OOK, PPM and pam modulation schemes for free space optical (FSO) communication systems: Analytical study," *Int. J. Comput. Appl.*, vol. 79, no. 11, pp. 22–27, Oct. 2013.

[10] G. A. Mahdiraji and E. Zahedi, "Comparison of selected digital modulation schemes (OOK, PPM and DPIM) for wireless optical communications," in *Proc. 4th Student Conf. Res. Develop.*, 2006, pp. 5–10.

[11] J. Shen et al., "Towards power-efficient long-reach underwater wireless optical communication using a multi-pixel photon counter," *Opt. Exp.*, vol. 26, no. 18, pp. 23565–23571, Aug. 2018.

[12] Q.-R. Yan, M. Wang, W.-H. Dai, and Y.-H. Wang, "Synchronization scheme of photon-counting underwater optical wireless communication based on PPM," *Opt. Commun.*, vol. 495, Sep. 2021, Art. no. 127024.

[13] J. Huang, C. Li, J. Dai, R. Shu, L. Zhang, and J. Wang, "Real-time and high-speed underwater photon-counting communication based on SPAD and PPM symbol synchronization," *IEEE Photon. J.*, vol. 13, no. 5, Oct. 2021, Art. no. 7300209.

[14] C. Zhang et al., "9.14-Mbps 64-PPM UWOC system based on a directly modulated MOPA with pre-pulse shaping and a high-sensitivity PMT with analog demodulation," *Opt. Exp.*, vol. 30, no. 17, pp. 30233–30245, Aug. 2022.

[15] R. Chen, Z. Lv, Y. Li, C. Qiu, and Z. Liu, "P-3.19: Demonstration of underwater wireless optical communication system using a green micro-LED and FPGA-based PPM modulation," in *Proc. SID Symp. Dig. Tech. Papers*, 2022, pp. 732–734.

[16] C. Zhang et al., "Theoretical analysis and experimental demonstration of gain switching for a PPM based UWOC system with picosecond pulses," *Opt. Exp.*, vol. 30, no. 21, pp. 38663–38673, Oct. 2022.

[17] S. Hu, L. Mi, T. Zhou, and W. Chen, "35.88 attenuation lengths and 3.32 bits/photon underwater optical wireless communication based on photon-counting receiver with 256-PPM," *Opt. Exp.*, vol. 26, no. 17, pp. 21685–21699, Aug. 2018.

[18] S. Zhu, X. Chen, X. Liu, G. Zhang, and P. Tian, "Recent progress in and perspectives of underwater wireless optical communication," *Prog. Quantum Electron.*, vol. 73, Jul. 2020, Art. no. 100274.

[19] S. Q. Duntley, "Light in the sea," *J. Opt. Soc. Amer.*, vol. 53, no. 2, pp. 214–233, Feb. 1963.

[20] K. Mamatha, K.B. N. S. K. Chaitanya, S. Kumar, and A. A. B. Raj, "Underwater wireless optical communication—A review," in *Proc. Int. Conf. Smart Gener. Comput., Commun. Netw.*, 2021, pp. 1–5.

[21] M. Kuznetsov, F. Hakimi, R. Sprague, and A. Mooradian, "High-power (>0.5-W CW) diode-pumped vertical-external-cavity surface-emitting semiconductor lasers with circular TEM_{00} beams," *IEEE Photon. Technol. Lett.*, vol. 9, no. 8, pp. 1063–1065, Aug. 1997.

[22] A. Tropper and S. Hoogland, "Extended cavity surface-emitting semiconductor lasers," *Prog. Quantum Electron.*, vol. 30, no. 1, pp. 1–43, Jan. 2006.

[23] A. Rahimi-Iman, "Recent advances in VECSELs," *J. Opt.*, vol. 18, no. 9, Oct. 2016, Art. no. 093003.

[24] M. Guina, A. Rantamäki, and A. Härkönen, "Optically pumped VECSELs: Review of technology and progress," *J. Phys. D: Appl. Phys.*, vol. 50, no. 38, Aug. 2017, Art. no. 383001.

[25] B. Rudin et al., "Highly efficient optically pumped vertical-emitting semiconductor laser with more than 20 W average output power in a fundamental transverse mode," *Opt. Lett.*, vol. 33, no. 22, pp. 2719–2721, Nov. 2008.

[26] B. Heinen et al., "106 W continuous-wave output power from vertical-external-cavity surface-emitting laser," *Electron. Lett.*, vol. 48, no. 9, pp. 516–517, Apr. 2012.

[27] C. D. Mobley et al., "Comparison of numerical models for computing underwater light fields," *Appl. Opt.*, vol. 32, no. 36, pp. 7484–7504, Dec. 1993.

[28] A. Laux et al., "The a, b, c s of oceanographic lidar predictions: A significant step toward closing the loop between theory and experiment," *J. Modern Opt.*, vol. 49, no. 3/4, pp. 439–451, Apr. 2002.

[29] P. Tian et al., "Absorption and scattering effects of maalox, chlorophyll, and sea salt on a micro-LED-based underwater wireless optical communication," *Chin. Opt. Lett.*, vol. 17, no. 10, Sep. 2019, Art. no. 100010.
[30] L. Mullen, A. Laux, and B. Cochenour, "Propagation of modulated light in water: Implications for imaging and communications systems," *Appl. Opt.*, vol. 48, no. 14, pp. 2607–2612, May 2009.
[31] B. Cochenour, K. Dunn, A. Laux, and L. Mullen, "Experimental measurements of the magnitude and phase response of high-frequency modulated light underwater," *Appl. Opt.*, vol. 56, no. 14, pp. 4019–4024, May 2017.
[32] A. Luchinin and V. Savel'Ev, "Propagation of a sinusoidally modulated light beam through a scattering medium," *Radiophys. Quantum Electron.*, vol. 12, no. 2, pp. 205–211, Feb. 1969.
[33] B. M. Cochenour and A. Laux, "Experimental validation of a Monte Carlo model for determining the temporal response of the underwater optical communications channel," *Proc. SPIE*, vol. 9459, pp. 15–23, 2015.
[34] C. Zheng and H. Shen, "Understanding nonlinear optical phenomenon for underwater material ablation by ultrafast laser with high pulse energy," *J. Manuf. Processes*, vol. 70, pp. 331–340, Sep. 2021.
[35] T. Wang et al., "15 Mbps underwater wireless optical communications based on acousto-optic modulator and NRZ-OOK modulation," *Opt. Laser Technol.*, vol. 150, Feb. 2022, Art. no. 107943.
[36] Z. Ghassemlooy, A. Hayes, N. L. Seed, and E. D. Kaluarachchi, "Digital pulse interval modulation for optical communications," *IEEE Commun. Mag.*, vol. 36, no. 12, pp. 95–99, Dec. 1998.

Liqi Liu is currently working toward the M.S. degree in optical engineering with Chongqing Normal University, Chongqing, China. His research focuses on underwater wireless optical communications.

Tao Wang received the B.S. degree in renewable resource science and technology from Yunnan Normal University, Kunming, China, in 2012, and the Ph.D. degree in condensed matter physics from the Changchun Institute of Optics, Fine Mechanics and Physics, Chinese Academy of Sciences, Changchun, China, in 2017. He is currently with Chongqing Normal University. His research interests include high beam quality diode lasers, semiconductor disk lasers, and underwater wireless optical communications.

Ruiyang Tian is currently working toward the M.S. degree in optical engineering with Chongqing Normal University, Chongqing, China. His research focuses on underwater wireless optical communications.

Renjiang Zhu received the B.S. degree in optical engineering from Chongqing Normal University, Chongqing, China, in 2006, and the Ph.D. degree in optical engineering from Chongqing University, Chongqing, in 2015. He is currently with Chongqing Normal University. His research interests include semiconductor disk lasers, ultrafast optics, and nonlinear optics.

Cunzhu Tong (Senior Member, IEEE) received the M.S. degrees in physics from Chongqing University, Chongqing, China, in 2002, and the Ph.D. degree in microelectronics and solid electronics from the Institute of Semiconductors, Chinese Academy of Sciences, Beijing, China, in 2005. From 2005 to 2009, he was a Research Fellow with Nanyang Technological University, Singapore. After that, he joined the Department of Electrical and Computer Engineering, University of Toronto, Toronto, ON, Canada, as a Postdoctoral Researcher. He became a Professor of Hundred Talents Program, Chinese Academy of Sciences (CAS) and was with the Changchun Institute of Optics, Fine Mechanics and Physics, CAS, Changchun, China, in November 2010. His research interests include Bragg reflection waveguide devices, photonic crystal lasers, mid-infrared lasers, and beam combining of diode lasers.

Lijie Wang received the B.S. degree in optical communications from Jilin University, Changchun, China, in 2008, and the Ph.D. degree in condensed matter physics from the Changchun Institute of Optics, Fine Mechanics and Physics, Chinese Academy of Sciences, Changchun, in 2013. He is currently with the Changchun Institute of Optics, Fine Mechanics and Physics, Chinese Academy of Sciences. His research interests include high brightness diode lasers, mid-infrared lasers, and photonic crystal lasers.

Yanrong Song received the B. S. degree in semiconductor physics from Tianjin University, Tianjin, China, in 1985, and the Ph.D. degree in optics from Shanxi University, Taiyuan, China, in 2000. She is currently a Professor with the Faculty of Science and the Head of the Photo-electronics Information Institute, Beijing University of Technology, Beijing, China. Her research interests include ultrafast optics, fiber lasers, novel semiconductor lasers, and nonlinear optics.

Peng Zhang received the M.S. and Ph.D. degrees in optics from the Beijing University of Technology, Beijing, China, in 2007 and 2010, respectively. He is currently with the Chongqing National Center for Applied Mathematics. His research interests include semiconductor disk lasers, ultrafast optics, nonlinear frequency conversion, and underwater wireless optical communications.